Adaptation of the Two-CAP method for conduction velocity distribution estimation in multi-channel recordings

Mafalda Ribeiro[1,2], Kamil Wozniak[3], Felipe Retore Andreis[4], Thomas Gomes Nørgaard dos Santos Nielsen[4], and Benjamin Metcalfe[1,2,3]

***Abstract*— Closed-loop neural interfaces capable of both stimulating and recording from peripheral nerves have the potential to enhance the long-term efficacy of neural implants. One challenge associated with closed loop interfaces is the accurate estimation of the distribution of active fibre conduction velocities (DCV) when recording the immediate effect of stimulation. DCV estimation has been performed in monopolar surface recordings using the Two-CAP method. This work extends the Two-CAP method and demonstrates its application to bipolar in-vivo recordings made with multiple-electrode arrays. A sensitivity analysis was conducted using simulated data with ground truth to ascertain the stability and limits of the algorithm before experimental data was examined. The sensitivity analysis highlighted that recording distance shows a considerable impact on the performance of this extended Two-CAP method, as well as the velocity interval chosen when creating the model. The in-vivo data was also compared against an equivalent simulated model, and a relatively low mean squared error was obtained when comparing the two distributions.**

I. INTRODUCTION

Conduction velocity (CV) studies in peripheral nerves have been essential for investigating both nerve function and health. By being able to identify the CVs contributing to a neural response, it is possible to determine whether particular fibre classes are active, inactive, or being excited or inhibited appropriately under a given stimulation profile. One of the main potential applications of these studies is early detection of peripheral neuropathy [1].

There are various approaches for recording neural activity in peripheral nerves with varying degrees of invasiveness. Approaches which do not penetrate the epinerium are typically referred to as being extraneural, and were originally conducted on the surface of the skin. More recently, implantable devices such as cuff electrodes which surround the nerve have also been used. Given the recording site, these approaches capture neural activity in the form of compound action potentials (CAPs), consisting of a combination of multiple individual single-fibre action potentials (SFAPs). Finding the different SFAP velocities contributing to a CAP recording is a problem that has been investigated predominantly from the perspective of monopolar surface recordings on the skin. Several methods have been proposed to achieve this, such as the Two-CAP method [1], the discrete spectrum method [2], and velocity-selective recording [3], [4]. The Two-CAP method in particular has been successfully used in the analysis of monopolar surface recordings and requires recordings of CAPs at two distinct locations along the nerve. An optimisation problem can then be devised for determining the distribution of SFAP conduction velocities (DCV) contributing to a pair of observed CAPs. The primary benefit of this technique is that no prior knowledge of SFAP waveforms is required.

In contrast with monopolar surface recording setups, implantable multi-electrode cuffs are typically configured in a bipolar or tripolar manner to minimise common-mode noise. Additionally, given that these devices are implanted in-vivo, the dimensions and electrode spacing are now in the order of tens of mm, as opposed to surface recordings which used distances in the order of cm. Therefore, a crucial gap in DCV estimation research is how to apply the Two-CAP method beyond two monopolar recordings. It also remains to be ascertained what the limits of the algorithm are in terms of experimental and model parameters. To the best of our knowledge, there is no algorithm for in-vivo multi-channel recordings that accurately quantifies the contribution of each SFAP CV class to the overall CAP response.

Thus, this paper introduces two key changes that enable the Two-CAP algorithm to be used in multi-channel bipolar in-vivo recordings. Furthermore, a sensitivity analysis is conducted using simulated data to ascertain the accuracy and boundaries of the extended Two-CAP model. Finally, the extended Two-CAP model is also applied for the first time to in-vivo recordings collected using a multi-electrode cuff implanted on the ulnar nerve of a pig. In the future, such an algortihm with minimal assumptions will be vital for investigating the CVs contributing towards a response in the nerve in-vivo, particularly beyond animal work where nerves cannot be investigated with highly invasive surgeries.

II. METHODS

A. Two-CAP model

When recording from a whole nerve extraneurally after electrical stimulation the activity obtained is a CAP, which comprises of overlapping individual single fibre action potentials (SFAPs). Within a recording, it can be assumed that there are up to N distinct velocity classes, each producing

[1]Centre for Accountable, Responsible, and Transparent AI (ART-AI), Department of Computer Science, University of Bath, BA2 7AY, UK

[2]Centre for Biosensors, Bioelectronics, and Biodevices (C3Bio), Department of Electronic & Electrical Engineering, University of Bath, BA2 7AY, UK

[3]Department of Electronic & Electrical Engineering, University of Bath, BA2 7AY, UK

[4]Center for Neuroplasticity and Pain (CNAP), Department of Health Science and Technology, Aalborg University, 9220 Aalborg, Denmark

SFAPs with different delays. A CAP can therefore be expressed as [5]:

$$C(t_k) = \sum_{i=1}^{N} w_i f_i(t_k - d_i) \tag{1}$$

Where $C(t_k)$ is the CAP at time t_k, i is a specified velocity class, and f_i, d_i, and w_i are the SFAP, propagation delay, and amplitude weighing coefficient for velocity class i, respectively. This equation can also be written in a more compact matrix form, as follows:

$$C = AQ\mathbf{w} \tag{2}$$

Where A is a matrix composed of all the unitary SFAP vectors, and Q is the velocity-dependent information for the SFAP. Assuming a constant SFAP shape across all velocity classes, each row in the Q matrix consists of all zeros, except for a one at the correct index to yield the delay d_i in the function $f_i(t_k - d_i)$.

When recording two CAPs, C_1 and C_2, at two distinct locations along the nerve, and following Equation 2, two distinct Q matrices are obtained, Q_1 and Q_2. Post-convolving the equations for C_1 and C_2 with $Q_2\mathbf{w}$ and $Q_1\mathbf{w}$, respectively, produces the following:

$$C_1 Q_2 \mathbf{w} = C_2 Q_1 \mathbf{w} \tag{3}$$

which implies:

$$[C_1 Q_2 - C_2 Q_1]\mathbf{w} = \phi \tag{4}$$

Where ϕ is the null vector. A solution for vector $\mathbf{w}$ can therefore be found using quadratic optimisation, as proposed by Cummins et al. [1]. Some key assumptions related to this method are that SFAP duration does not change significantly over the range of velocities considered, the amplitude contribution to each CV class is proportional to the number of fibres in that class, and with long conduction distances, activation time and virtual cathode effects were considered to be minimal. Beyond these, this approach has the key benefit of not requiring any prior information about the A matrix, or the SFAP shape, when conducting the optimisation process, making it ideal for extraneural recordings such as those conducted with cuffs.

B. Extensions to Two-CAP model

The experimental work conducted with the original Two-CAP model focused primarily on surface, monopolar recordings. As previously described, recent neuromodulation devices such as multi-electrode cuffs are now implantable and consist of multiple recording channels, configured in bipolar or tripolar configurations to minimise common-mode noise. These devices also now cover much shorter distances, in the order of tens of mm, compared to surface recordings that have inter-electrode distances typically in the order of cm. Therefore, the Two-CAP approach requires two key modifications prior to being applied to these recordings.

The first change is in the Q matrix generation stage, where there may now be several recording sites associated with a single channel recording. Using the example of a bipolar recording, this consists of a differential recording between two physical electrodes, therefore, two Q matrices are calculated per CAP. Equation 2 then becomes:

$$C = A(Q_{i+1} - Q_i)\mathbf{w} \tag{5}$$

Where Q_i is the Q matrix for the ith electrode and Q_{i+1} is the same for the electrode immediately after. This also changes the minimisation problem to the following:

$$[C_1(Q_{j+1} - Q_j) - C_2(Q_{i+1} - Q_i))]\mathbf{w} = \phi \tag{6}$$

Where Q_j and Q_{j+1} are associated with the second CAP, C_2, and have analogous relationships to those described for the Q matrices for the first CAP, C_1. Equation 6 therefore summarises the changes required for applying the Two-CAP method to bipolar recordings. This can be readily modified to support tripolar recordings or more by adding a corresponding amount of Q matrices and replicating the recording polarities.

The second proposed change relates to how the algorithm handles data from multiple channels. In this case, the chosen approach is to loop through pairs of adjacent electrodes and perform the Two-CAP estimation on each pair. This produces multiple estimates for the $\mathbf{w}$ vector, which can be averaged to produce a final estimate for the DCV. Following this approach with multiple recording sites also provides the benefit of decreased noise in the DCV estimation given that calculating the w vector for multiple pairs results in uncorrelated noise being averaged out at the end of the process.

C. Data collection

1) Simulated data: Simulated data was based on generating SFAPs using a transmembrance AP (TMAP) model, described mathematically as follows:

$$a(t, t_0) = \max(A(t - t_0)^n e^{-B(t-t_0)}, 0) \tag{7}$$

Where t_0 is the time at which the AP occurs, and the constants A, B, and n were set to 2.2e7, 7.2e3, and 3, respectively. This produced an SFAP with an amplitude of $80\,\mu\mathrm{V}$ and duration of $2\,\mathrm{ms}$. Ten bipolar CAPs were then generated by adding delayed SFAPs according to a specified distribution. In this case, both a unimodal and more complex bimodal distribution were considered, to illustrate the examples of nerves containing one predominant conduction velocity or two.

2) Experimental data: An experimental in-vivo recording from pig ulnar nerve was also used to validate the extended Two-CAP model. The recording was conducted using a multi-electrode cuff with 11 recording channels, and electrical stimulation was performed using a tripolar stimulation cuff, both containing platinum-iridium electrodes. The

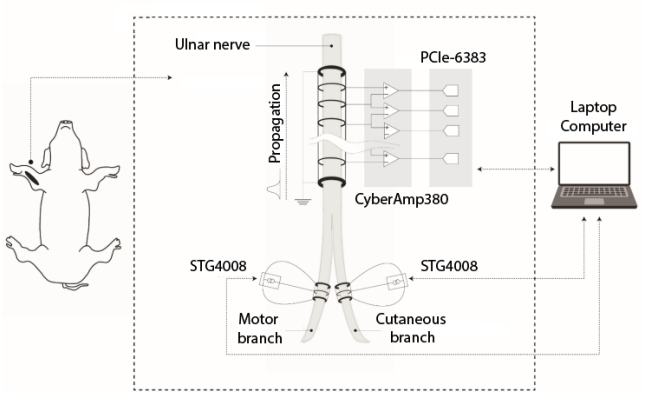

Fig. 1. Setup used for collecting in-vivo pig ulnar nerve recordings, including electronic apparatus used to conduct tripolar stimulation and bipolar recordings at the ulnar nerve. Electrical stimulation was conducted at the motor and cutaneous branches using programmable stimulators (STG4008), and the response recorded across the entire nerve using amplifiers (CyberAmp380) and a data acquisition card (PCIe-6383). This diagram was adapted with permission from Felipe Rettore Andreis et al., Sensors; published by MDPI in 2022 [6].

recording cuff was approximately $50\,\mathrm{mm}$ long and the inter-electrode spacing was $3.5\,\mathrm{mm}$. Surgical protocols were described in prior publications [6]. Charge-balanced, biphasic current stimulation was used, with amplitudes ranging from 0 to $10\,\mathrm{mA}$, and a peak charge density of $24.5\,\mu\mathrm{C\,cm^{-2}}$. On the recording side, the mean amplifier gain was 75 dB, and the recordings were bandpass filtered using a fourth order Bessel filter from $100\,\mathrm{Hz}$ to $10\,\mathrm{kHz}$.

D. Sensitivity Analysis

In order to investigate the limits of the extended Two-CAP method and the variation in predicted DCVs, relevant experimental and model parameters were swept across a range of values when examining both unimodal and bimodal simulated data. On the experimental side, it has been previously hypothesised that smaller stimulation and recording distances produce less accurate DCV estimations, however, the exact limit has not yet been determined or investigated, particularly when considering multi-electrode cuff recordings [7]. Additionally, when running the extended Two-CAP algorithm, a histogram is produced, which requires setting up expected velocity ranges and bin widths (steps) a priori. This, in turn, might also affect the accuracy of the estimated DCV.

A set of default values were produced in the same order of magnitude as prior surface recordings which have been previously used with the original Two-CAP method [8], and each individual parameter was then swept across a range of values, specified in Table I. The parameters include (1) the distance between the stimulation and first recording site, (2) the distance between individual recording sites, (3) the velocity steps in the DCV histogram, and (4) the minimum and maximum limits of the DCV. This process was repeated for unimodal and bimodal distributions, to highlight whether the distribution shape itself affects the estimated DCV.

Given that this analysis was conducted using simulated data with a known ground truth DCV, the mean squared error (MSE) was calculated between original and estimated DCVs and used to quantify the performance of the extended Two-CAP method for each parameter range. Reconstructed CAPs were also generated for a more qualitative analysis of the results.

TABLE I

OVERVIEW OF EXPERIMENTAL AND MODEL PARAMETERS CONSIDERED FOR THE SENSITIVITY ANALYSIS OF THE EXTENDED TWO-CAP METHOD

Parameter	Default value	Range
Stimulation distance (cm)	10	0.1 - 10
Recording site distance (cm)	3.5	0.01 - 10
DCV velocity step size (m/s)	1	0.5 - 5
DCV minimum velocity (m/s)	10	5 - 30
DCV maximum velocity (m/s)	100	40 - 120

The results from this sensitivity analysis were then used to inform suitable experimental and model parameters to use when applying the extended Two-CAP method to data collected from a pig ulnar nerve in-vivo using a multi-electrode cuff.

III. RESULTS

A. Sensitivity analysis

The extended Two-CAP algorithm was initially applied to simulated bipolar CAP data, generated as described in Section II-C and a sensitivity analysis was conducted to ascertain the effect of (1) the distance from the first recording electrode to the stimulation site, (2) the distance between recording electrodes, (3) the velocity steps, and (4) the minimum and maximum limits of the DCV. The MSE was calculated for each parameter sweep.

1) Comparing unimodal to bimodal distributions: The two simulated datasets consisted of CAPs derived from a unimodal distribution around $55\,\mathrm{m\,s^{-1}}$, and another from a bimodal distribution with modes of 32 and $78\,\mathrm{m\,s^{-1}}$. The unimodal distribution and corresponding CAPs are shown in Figure 3A and C, and the equivalent plots for the biomdal distribution is shown in subfigures B and D. These were generated using the default parameters described in Table I, namely a velocity range from 10 to $100\,\mathrm{m\,s^{-1}}$ in steps of $1\,\mathrm{m\,s^{-1}}$, a stimulation distance of $10\,\mathrm{cm}$ and a distance between recording sites of $3.5\,\mathrm{cm}$. A bipolar configuration with ten channels was used similarly to the cuff configuration previously shown in Figure 1 where adjacent bipolar recordings share a common recording site.

The two-CAP algorithm was applied to both the unimodal and bimodal distribution CAPs, and the estimated distribution ($\mathbf{w}$ vector) compared against the ground truth using MSE. For the unimodal case, an MSE of 4.39×10^{-6} was obtained, whereas the bimodal case yielded an MSE of 2.51×10^{-6}. The results from this sensitivity analysis were summarised in Figure 2.

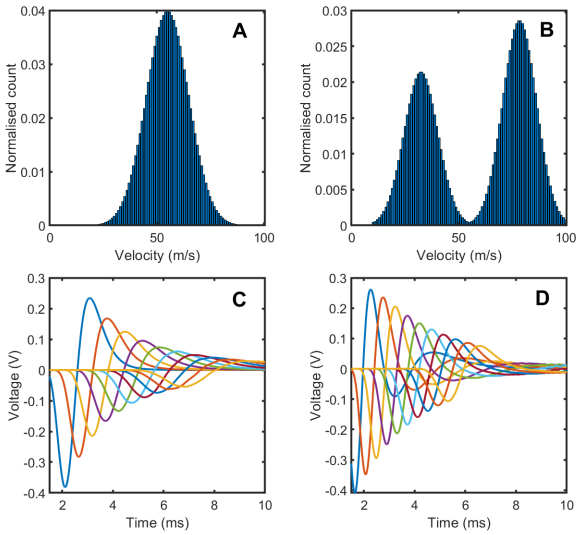

Fig. 3. Simulated data distributions and corresponding CAPs generated using default parameters from Table I. **(A)** Normalised unimodal distribution, **(B)** Normalised bimodal distribution, **(C)** Resultant CAPs from TMAP model and unimodal distribution, and **(D)** Resultant CAPs from TMAP model and bimodal distribution.

After this stage, different parameters were varied across a range of physiologically plausible values for neural recordings to assess the variability in performance when changing various experimental and model parameters.

2) Effect of stimulation distance: Depending on the application, the distance from the stimulation site to the first recording site can be as small as a few millimetres, or as large as a few centimetres. Therefore, a sweep of 0.1-10 cm was conducted, which highlighted only slight variation in MSE for increasing stimulation distance, both for unimodal and bimodal fibre distributions.

3) Effect of distance between recording sites: Similarly to stimulation distance, the distance between recording sites can also vary significantly depending on the approach used for conducting recordings. A sweep of values ranging from 0.01 to 10 cm was done, which showed a very prominent trend of decreasing MSE with increasing distance between recording sites. Given the significant difference in MSE and distribution estimation between 0.01 and 2.5 cm, a narrower search was conducted up to 50 mm to ascertain the minimum separation between recording electrodes to achieve a similar performance to the one at 2.5 cm. At recording distances of 15 mm or larger, the MSE becomes $\leq 9.64 \times 10^{-6}$. This is also highlighted in Figure 4, where A-E are increasing recording distances from 0.01 to 3 cm, and the underlying ground truth is shown as a red line on each plot This is the range also used in the bar plot in Figure 2B.

4) Effect of varying velocity step: Beyond experimental parameters, there are also model parameters relating to the extended Two-CAP method specifically which need to be set prior to running the algorithm. One of these is the velocity steps in which to discretise the DCV. Therefore, this parameter was swept from 0.5-5 $\mathrm{m\,s^{-1}}$. This highlighted that smaller velocity steps produce lower MSEs.

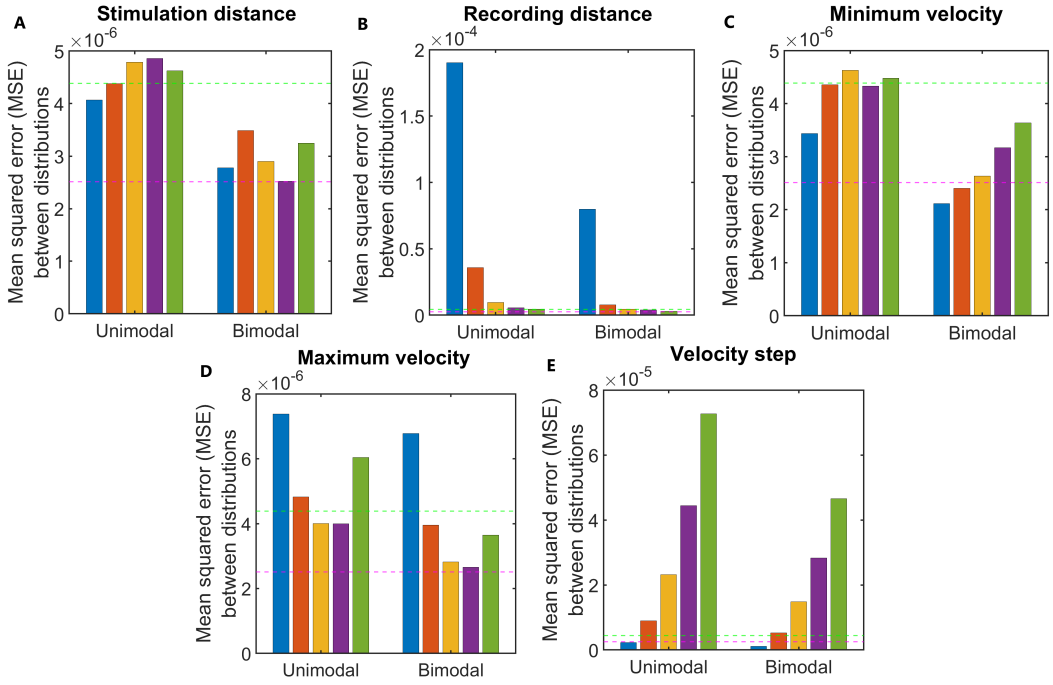

Fig. 2. Bar graphs highlighting changes in MSE for unimodal and bimodal CV distributions when varying different parameters. Dashed horizontal lines were included in all graphs to show how results using default values compare (with the green line corresponding to unimodal, and magenta to bimodal MSEs). In each graph, the values for each parameter increase from left to right **(A)** Effect of sweeping stimulation distance from 0.1 to 10 cm. **B** Effect of sweeping recording distance from 0.01 to 3 cm. **C** Effect of minimum velocity from 5 to 30 $\mathrm{m\,s^{-1}}$. **D** Effect of maximum velocity from 40 to 120 $\mathrm{m\,s^{-1}}$. **E** Effect of velocity step from 0.5 to 5.

5) Effect of changing velocity ranges: Finally, the minimum and maximum velocities for composing the inital simulated CAPs and subsequently used as boundaries for the extended Two-CAP were also varied. The main aim behind this was to ascertain whether narrower ranges of velocities contributing towards the response affect the accuracy of the algorithm. The minimum velocity was swept from 5-30 $\mathrm{m\,s^{-1}}$, and the maximum velocity from 50-120 $\mathrm{m\,s^{-1}}$. The MSEs obtained highlighted that the maximum velocity limit had the largest impact, with larger values up to 100 $\mathrm{m\,s^{-1}}$ producing lower MSEs.

B. In-vivo pig ulnar recording

The extended Two-CAP algorithm was subsequently applied to one in-vivo pig ulnar recording without a known SFAP fibre diameter distribution. In this case, the experimental parameters were a stimulation distance of 44 mm and inter-electrode spacing of 3.5 mm. The velocity range to be searched through was set to a range of 10-75 $\mathrm{m\,s^{-1}}$ in steps of 1 $\mathrm{m\,s^{-1}}$. These boundaries were informed by prior ranges reported in the literature for the specific animal and nerve [6]. Given the availability of multiple recording sites, the Two-CAP algorithm was calculated for each pair, and a mean estimated distribution was obtained.

Figure 5A shows example CAPs recorded from the pig ulnar nerve after stimulating the motor branch. When applying the extended Two-CAP method to this data, the distribution shown in Figure 5B was obtained. This distribution was scaled by a factor of v^2 to account for the fact that the recording was conducted using a multi-electrode cuff, which poses an additional nerve-electrode transfer function [9]. When running a simulated model with the same experimental parameters, an MSE of 2.6×10^{-4} was obtained when comparing the Two-CAP distributions for both simulated and experimental data.

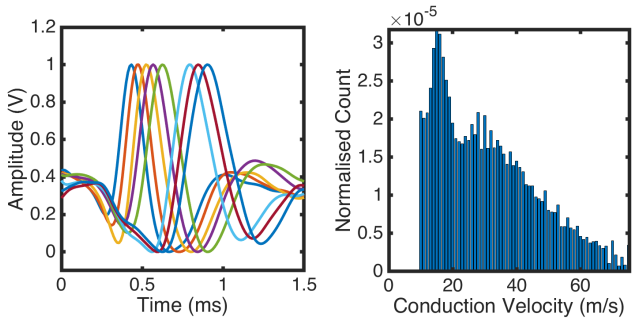

Fig. 5. Bipolar CAPs from in-vivo data from pig ulnar nerve and corresponding distributions from Two-CAP method. **(A)** Plot of original CAP recordings in the time domain at supramaximal stimulation levels (10 mA) **(B)** Estimated DCV using Two-CAP method.

IV. DISCUSSION

In this paper, changes to the Two-CAP method were proposed to support multi-channel bipolar recordings. In addition to this, a sensitivity analysis was conducted to ascertain the stability and limits of the Two-CAP algorithm at a range of experimental and model parameters. Finally, the algorithm was also applied to an in-vivo recording and compared against a simulated recording with the same experimental parameters.

For the sensitivity analysis, two types of CAPs were generated using a TMAP model. The CAPs derived from a unimodal distribution in general showed a slightly higher MSE than those derived from a bimodal distribution.

In terms of experimental parameters, both the distances between the stimulation and first recording site, and between recording sites, showed changes in MSE between estimated and ground truth DCVs. In the case of increasing stimulation distances, there was no significant trend in MSE. A limitation

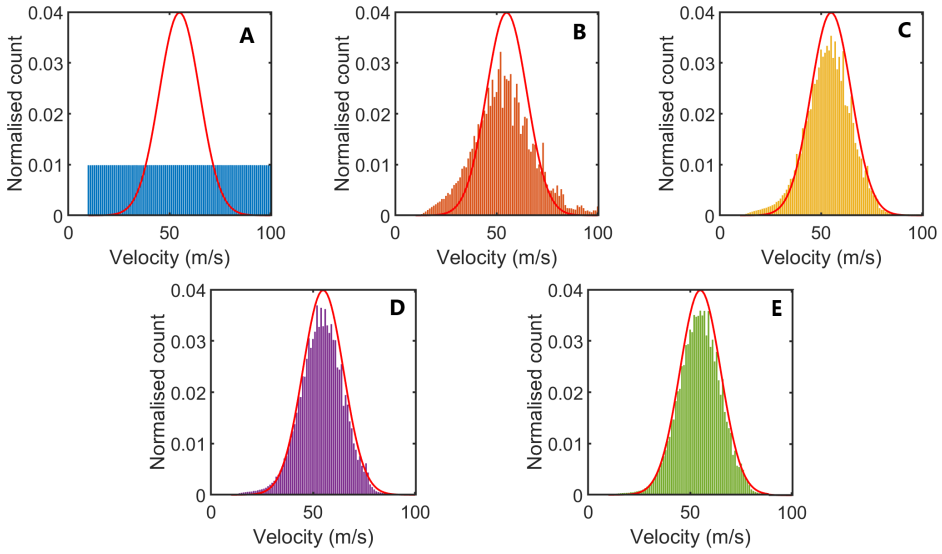

Fig. 4. Effect of increasing recording distance, with results shown for unimodal data and inter-electrode distances of **(A)** 0.01 cm, **(B)** 0.75 cm, **(C)** 1.5 cm, **(D)** 2.25 cm, **(E)** 3 cm. The ground truth distribution is overlaid on each plot as a red line.

potentially worth considering in this simulation model is that stimulation effects, such as artefacts, are not included in the recording. In future work, it would therefore be valuable to apply this model to CAPs from a biophysical simulation tool, to more accurately model the effects of neural stimulation. In the case of recording distances, decreasing the distance below $15\,\mathrm{mm}$ decreased the MSE significantly, with larger distances having lower MSEs and the distributions more closely matching the group truth (see Figure 4). This is in agreement with prior studies conducted using monopolar setups which used recording distances in the order of cm to ensure there is sufficient change in CAP waveform to discriminate between CVs and to minimise the virtual cathode effect [1].

Model parameters such as velocity step and the overall velocity range to be searched through were also analysed. These showed that the velocity step in producing the discretised histogram is a crucial contributor to the MSE, and hence performance, of the Two-CAP algorithm. The velocity range also showed that the extended Two-CAP algorithm with multiple recording sites tends to perform better at wider velocity ranges.

Finally, the extended Two-CAP model was also applied to an in-vivo pig ulnar recording. The results from this were compared against a simulated model with replicated experimental and model parameters, which yielded an MSE of 2.6×10^{-4} when comparing the experimental distribution to its simulated counterpart.

V. CONCLUSIONS

This paper outlined how to expand the original Two-CAP algorithm so it can be applied to bipolar configurations, as well as multi-electrode recordings. This was motivated by currently ongoing research into implantable neural interfaces, such as cuffs, for which there are yet to be any techniques for accurately decomposing a CAP into a DCV. A sensitivity analysis was conducted to ascertain which experimental and model parameters have most effect on predicted distributions, and it was found that recording distance was a key contributor. From the model side, the velocity step used also significantly influenced the accuracy of the predicted distribution. Finally, an in-vivo dataset with no ground truth distribution was also included, and compared against an equivalent simulated TMAP model. A close agreement was seen between the two distributions. Future work for developing this algorithm includes using a more complex, biophysical simulation model, as well as validating the results with multiple animal recordings.

To conclude, this approach would be a crucial addition to analysis techniques commonly used for in-vivo recordings, given that identifying DCVs assists in identifying and classifying different types of nerve function, such as motor, sensory, and autonomic. Hence, potential applications for this work include closed-loop peripheral nerve interfaces for effectively restoring sensory and motor function, or treatment of different disorders of the peripheral nervous system by verifying that specific fibre velocities, or diameters, are activated or inhibited.

REFERENCES

[1] K. L. Cummins, L. J. Dorfman, and D. H. Perkel, "Nerve fiber conduction-velocity distributions. II. Estimation based on two compound action potentials," *Electroencephalography and Clinical Neurophysiology*, vol. 46, no. 6, pp. 647–658, 1979.

[2] G. Hirose, Y. Tsuchitani, and J. Huang, "A new method for estimation of nerve conduction velocity distribution in the frequency domain," *Electroencephalography and Clinical Neurophysiology*, vol. 63, no. 2, pp. 192–202, 1986.

[3] J. Taylor, M. Schuettler, C. Clarke, and N. Donaldson, "The theory of velocity selective neural recording: A study based on simulation," *Medical and Biological Engineering and Computing*, vol. 50, no. 3, pp. 309–318, 2012.

[4] B. Metcalfe, T. Nielsen, and J. Taylor, "Velocity Selective Recording: A Demonstration of Effectiveness on the Vagus Nerve in Pig," *Proceedings of the Annual International Conference of the IEEE Engineering in Medicine and Biology Society, EMBS*, vol. 2018-July, pp. 2945–2948, 2018.

[5] K. L. Cummins, L. J. Dorfman, and D. H. Perkel, "Nerve fiber conduction-velocity distributions. I. Estimation based on two compound action potentials," *Electroencephalography and Clinical Neurophysiology*, vol. 46, no. 6, pp. 634–646, 1979.

[6] F. R. Andreis, B. Metcalfe, T. A. M. Janjua, W. Jensen, S. Meijs, and T. G. N. dos Santos Nielsen, "The Use of the Velocity Selective Recording Technique to Reveal the Excitation Properties of the Ulnar Nerve in Pigs," *Sensors*, vol. 22, no. 58, dec 2022. [Online]. Available: https://www.mdpi.com/1424-8220/22/1/58

[7] A. R. Liss, *Conduction velocity distributions: a population approach of electrophysiology of nerve*, L. J. Dorfman, K. L. Cummins, and L. J. Leifer, Eds. New York: Alan R. Liss Incorporated, 1983.

[8] K. L. Cummins and L. J. Dorfman, "Nerve fiber conduction velocity distributions: Studies of normal and diabetic human nerves," *Annals of Neurology*, vol. 9, no. 1, pp. 67–74, 1981.

[9] J. T. Taylor, N. Donaldson, and J. Winter, "Multiple-electrode nerve cuffs for low-velocity and velocity-selective neural recording," *Medical and Biological Engineering and Computing*, vol. 42, no. 5, pp. 634–643, 2004.